

# Discovery of an OB Runaway Star Inside SNR S147

B. Dinçel<sup>1\*</sup>, R. Neuhäuser<sup>1</sup>, S. K. Yerli<sup>2</sup>, A. Ankaý<sup>3</sup>, N. Tetzlaff<sup>1</sup>, G. Torres<sup>4</sup>, M. Mugrauer<sup>1</sup>

<sup>1</sup> *Astrophysikalisches Institut und Universitäts-Sternwarte Jena, 07745 Jena, Germany*

<sup>2</sup> *Orta Dođu Teknik Üniversitesi, Department of Physics, 06531 Ankara, Turkey*

<sup>3</sup> *Boğaziçi University, Department of Physics, 34342 İstanbul, Turkey*

<sup>4</sup> *Harvard-Smithsonian Center for Astrophysics, 60 Garden St., Mail Stop 20, Cambridge MA 02138, USA*

Accepted 2015 January 17. Received 2014 December 12; in original form 2014 May 25

## ABSTRACT

We present first results of a long term study: Searching for OB–type runaway stars inside supernova remnants (SNRs). We identified spectral types and measured radial velocities (RV) by optical spectroscopic observations and we found an early type runaway star inside SNR S147. HD 37424 is a B0.5V type star with a peculiar velocity of  $74 \pm 8 \text{ km s}^{-1}$ . Tracing back the past trajectories via Monte Carlo simulations, we found that HD 37424 was located at the same position as the central compact object, PSR J0538+2817,  $30 \pm 4$  kyr ago. This position is only  $\sim 4$  arcmin away from the geometrical center of the SNR. So, we suggest that HD 37424 was the pre–supernova binary companion to the progenitor of the pulsar and the SNR. We found a distance of  $1333^{+103}_{-112}$  pc to the SNR. The zero age main sequence progenitor mass should be greater than  $13 M_{\odot}$ . The age is  $30 \pm 4$  kyr and the total visual absorption towards the center is  $1.28 \pm 0.06$  mag. For different progenitor masses, we calculated the pre–supernova binary parameters. The Roche Lobe radii suggest that it was an interacting binary in the late stages of the progenitor.

**Key words:** OB Runaway Stars; HD 37424, Neutron Stars; pulsars; PSR J0538+2817, Supernova Remnants; SNR S147

## 1 INTRODUCTION

High space velocities of OB runaway stars are explained by two independent mechanisms: dynamical ejection due to gravitational interactions of massive stars in cluster cores (Poveda et al. 1967) and binary disruption as a result of a supernova explosion of the initially more massive component (Blaauw 1961). Both scenarios are viable, but whether one of the mechanisms is dominant is still uncertain. According to the virial theorem, through a symmetric supernova explosion in a binary system, if more than half of the total mass of the system is released, then the new born neutron star (or black hole) and the non–degenerate component are no more gravitationally bound (Blaauw 1961). However, the energy stored in the orbit, in most cases, is not sufficient to produce the neutron star kick velocities that are typically in the range of  $300\text{--}500 \text{ km s}^{-1}$  (Lyne & Lorimer 1994; Allakhverdiev et al. 1997; Hobbs et al. 2005; Hansen & Phinney 1997). The asymmetry in supernova explosions is responsible for such high velocities (Wongwathanarat et al. 2013). Therefore, there are no pulsar companions to many of the OB runaway stars (Sayer et al. 1996). In some cases, the compact object does not receive a significant kick and/or the majority of the total mass is stored on the secondary through conservative mass transfer, hence, the compact object remains bound to the companion star (van den Heuvel 1993). The runaway high mass X–ray

binaries like 4U1700–37 (Ankaý et al. 2001) and Vela X–1 (Kaper et al. 1997) are such examples.

Yet, the low rate of X–ray binaries and the high rate of isolated neutron stars by taking into consideration the selection effects, the binary disruption is likely to occur in most cases (Guseinov et al. 2005) (hereafter, G05). The kinematics of the binary disruption due to an asymmetric supernova explosion is widely discussed in Tauris & Takens (1998). However, a sample of observationally confirmed OB runaway–NS couples is needed for a better understanding of the problem.

The importance of searching for OB runaways inside SNRs was first mentioned in van den Bergh (1980). However, the kinematical study of known OB stars inside SNRs was concluded with a lack of OB runaways due to the poor sample of SNRs and OB stars. Still, there is no known O or B–type runaway star that can be directly linked to an SNR given in the literature.

In G05, the outcome of exploring runaway pairs from binary supernova disruption is broadly discussed. Firstly, identifying the explosion centers more precisely will be useful for determining the velocities of young NSs of which proper motion measurements have high uncertainties. Thus, the kick that is gained by the NS due to the asymmetry of the SN can be determined more precisely. Secondly, the distance to the remnant can be measured more accurately by studying the runaway star, as it cannot move far away from the explosion center in the observational lifetime of the SNR. Finally, possible effects of a close binary system on the asymmetry

\* Correspondence address: baha.dinçel@uni-jena.de

of the SNe can also be examined. Additionally, it would be a direct evidence of the binary supernova scenario (BSS).

The observational efforts are concentrated on runaway–NS coupling and abundance investigations of runaway stars. Some examples of the runaway–NS pairs (components are separated) are PSR B1929+10 –  $\zeta$  Oph (Hoogerwerf et al. 2001; Bobylev 2008; Tetzlaff et al. 2010), PSR J0630-2834 – HIP 47155 (Tetzlaff et al. 2013) and PSR J0826+2637 – HIP13962 (Tetzlaff et al. 2014). Based on their motions in space, the pulsars and the corresponding runaway stars were traced back in time by using 3–D Monte Carlo simulations. They were found at the same position and the same time inside a young open cluster. The PSR J0630-2834 – HIP 47155 pair is thought to be ejected from very old SNR Antlia.

There are considerable uncertainties in these cases as the supernova events took place more than  $10^5$  yr ago. The separation between the objects is very large and the SNR has faded away long ago and/or the components are outside of the SNR (the Antlia case). Other important observational evidence is the enhancement of  $\alpha$ -process elements in the hyper-velocity star HD 271791. The star is proposed to be ejected from a massive close binary system due to an SN that enriches its photosphere in elements which can be synthesized in large amounts during the evolution of the progenitor (Przybilla et al. 2008).

The method followed in our work is a direct study of possible runaway stars inside SNRs as described in G05.

Briefly, assuming that the massive binary mass ratio is greater than 1:4, OB-type star candidates are determined by a careful study of their BVJHK magnitudes obtained from the UCAC4 catalog (Zacharias et al. 2012). The angular separation of the sources from the geometrical centers of the remnants are within the limits of the maximum angular distance that a runaway star can have in a lifetime of an SNR. The distance moduli are calculated for all sources within this region, and the sources having extinctions and radial distances consistent with those of the SNRs are considered as "candidates". Measuring the radial velocities and identifying the spectral types of these objects via spectroscopy reveal their runaway nature, their youth and the exact spatial relations with the SNRs, in other words, the genetic connections.

Although the runaway stars arising from BSS may also be late type stars, it is time consuming to check the possible runaway nature of all the stars inside each SNR. Also, the late type stars are too faint to observe at large distances. A star having the same age as a supernova progenitor must be young. As OB type stars evolve faster, they automatically satisfy this condition. Furthermore, high mass stars are rare objects. An OB runaway star discovered inside an SNR can be explained by the BSS. Considering the very short observable lifetimes of SNRs and relatively short later evolution stages of stars, most probably, main sequence stars are expected as OB runaways connected to SNRs.

The space velocity of an OB runaway star is thought to be larger than  $30\text{--}40\text{ km s}^{-1}$  (Feast & Shuttleworth 1965; Sayer et al. 1996). A more precise value is proposed in Tetzlaff et al. (2011);  $28\text{ km s}^{-1}$  in 3–D and  $20\text{ km s}^{-1}$  in 2–D. To summarize, a main-sequence OB type star of which at least one component of the velocity vector is greater than  $20\text{ km s}^{-1}$  is searched in selected SNRs.

The first criterion of the candidate selection is the restriction of the angular position. Most of the OB runaways have peculiar velocities lower than  $80\text{ km s}^{-1}$  (Gies & Bolton 1986; Philp et al. 1996; Tetzlaff et al. 2011). As the shock wave velocity of the SNRs are decelerated from roughly  $10000\text{ km s}^{-1}$  to several hundred  $\text{km s}^{-1}$ , it is expected that the runaway star cannot exceed one tenth of the

**Table 1.** Distance estimates for S147. ( $R^l$ ) denotes the radius lower limit of the SNR.

Distance (kpc)	Method	Reference
$1.6\pm 0.3$	$\Sigma$ –D	Sofue et al. (1980)
$0.8\text{--}1.37$	$R^l$ , $\Sigma$ –D	Kundu et al. (1980)
0.6	$R^l$	Kirshner & Arnold (1979)
0.9	$\Sigma$ –D	Clark & Caswell (1976)
$0.8\pm 0.1$	$A_V$	Fesen et al. (1985)
1.06	$\Sigma$ –D	Guseinov et al. (2003)
$0.88<$	High Vel Gas	Sallmen & Welsh (2004)
1.2	Pulsar DM	Kramer et al. (2003)
$1.47^{+0.42}_{-0.27}$	Pulsar Plx	Ng et al. (2007)
$1.3^{+0.22}_{-0.16}$	Pulsar Plx	Chatterjee et al. (2009)

angular diameter ( $\theta$ ) of the related SNR. This value is somewhat relaxed to  $\theta/6$  considering the uncertainties in the geometrical centers of the SNRs. The stars in this region are expected to be consistent with the respective SNR in terms of distance and reddening.

For this comparison, the adopted distances of SNRs given in Guseinov et al. (2003, 2004a,b), and  $A_V$  values from Neckel et al. (1980) were used. 48 SNRs within 5 kpc from the Sun were selected for investigation.

In this paper, the result of the runaway search in SNR G180.0-1.7 (S147) is given. The kinematic relation between the runaway star HD 37424 and the pulsar PSR J0538+2817 is shown, the possible host OB association is discussed, the SNR parameters are constrained and the pre-supernova binary is constructed.

## 2 S147, PSR J0538+2817 AND HD 37424

S147 is a shell type SNR located in the Galactic anti-center direction. It is 180 arcmin in diameter with a geometrical center (GC) at  $\alpha = 05\text{h}39\text{m}00\text{s}$ ,  $\delta = +27^\circ 50'00''$  (Green 2009). It was first mentioned as an SNR candidate in Minkowski (1958). The compact object related to the SNR is radio pulsar PSR J0538+2817 (Anderson et al. 1996). In optical bands, the shell structure is well defined and dominated by filamentary emission in  $H\alpha$ . The emission is brighter in the north and south edges and mainly concentrated in the southern parts. Despite of its old age, it conserves the spherical symmetry except for the blowout regions in east and west (Figure 1). The total absorption in the V band is  $A_V=0.7 \pm 0.2$  magnitude (Fesen et al. 1985). Radio observations reveal that the spectral index is unusually varying. The shell structure observed at radio wavelengths coincides with that in optical bands and is well defined (Fuerst & Reich 1986). But, no X-ray emission is observed from the remnant (Sauvageot et al. 1990). Suggested distances vary from 0.6 to 1.9 kpc in various publications (Table 1). Four of the measurements are based on  $\Sigma$ –D relation which is useful to estimate the distance by using the surface brightness of the SNR. In Sofue et al. (1980) and Kundu et al. (1980), the model of Milne (1979) is used, while in Clark & Caswell (1976) and Guseinov et al. (2003), estimations are based on their own models. The radius lower limit calculated through SNR dynamics based on the model of Chevalier (1974) sets another constraint on the SNR distance. The distance derived from the pulsar's parallax or dispersion measure is larger than the distance suggested for the background stars of which spectra show high velocity gas related to the SNR.

The age was estimated as more than 100 kyr from the Sedov solution by using a shock velocity  $\sim 80\text{--}100\text{ km s}^{-1}$  (Sofue et al. 1980; Kundu et al. 1980). This velocity was derived from the RV

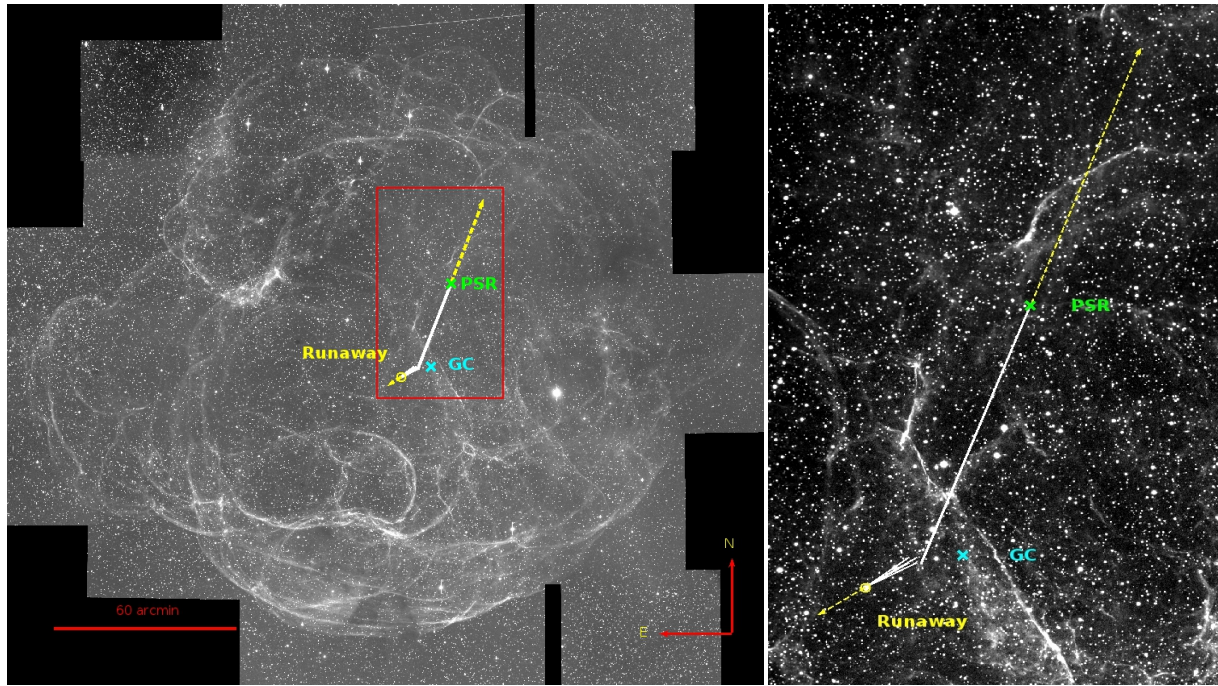


**Figure 1.** The  $4.8^\circ \times 4.1^\circ$  H $\alpha$  image of SNR S147 taken at the University Observatory Jena. The green cross represents the pulsar, the cyan cross shows the GC of the SNR and the yellow circle is HD 37424. The yellow vectors show the proper motion of the objects. The red box is the zoom-in area shown in the right panel. The white arrows are the tracing back cones of the proper motion for 29300 yr. The angle between the pm vectors is  $139^\circ - 148^\circ$ . In 2-D calculations, both objects come towards each other as close as 0.126 pc which means that they have a common origin; binary supernova disruption.

of the filamentary knots in [Lozinskaya \(1976\)](#); [Kirshner & Arnold \(1979\)](#). However the pulsar–SNR relation indicates an age of  $30 \pm 4$  kyr (from the travel time from the GC to the present position) ([Kramer et al. 2003](#); [Ng et al. 2007](#)). For a distance of 1.3 kpc, and an angular diameter of 200 arcmin, the radius (R) of the SNR is 38 pc. Then, assuming an age of 30 kyr, the remnant is in its Sedov Phase having a blast wave velocity of  $500 \text{ km s}^{-1}$ . The estimated explosion energy is between  $1-3 \times 10^{51}$  erg and the corresponding inter–cloud gas density is  $0.03-0.1 \text{ cm}^{-3}$  ([Katsuta et al. 2012](#)). The SNR is expanding in a low density medium, probably in the cavity generated by the progenitor.

The central source, PSR J0538+2817, is an extensively studied radio and X–ray pulsar located at  $\alpha = 05\text{h}38\text{m}25.1\text{s}$ ,  $\delta = +28^\circ 17'09.2''$ ,  $\sim 28$  arcmin away from the GC towards north. The 143.16 ms period and  $3.67 \times 10^{-15} \text{ s s}^{-1}$  period derivative ([Anderson et al. 1996](#)) imply a characteristic age of  $\sim 620$  kyr which is  $\sim 20$  times larger than its kinematic age of 30 kyr. This discrepancy is explained by either a long initial spin period of  $P_0 = 139$  ms ([Kramer et al. 2003](#)) or strong magnetic field decay ([Guseinov et al. 2004c](#)). The parallax distance was measured as  $1.47^{+0.42}_{-0.27}$  kpc ([Ng et al. 2007](#)) and  $1.3^{+0.22}_{-0.16}$  kpc ([Chatterjee et al. 2009](#)) and the dispersion measure (DM) distance is 1.2 kpc ([Kramer et al. 2003](#)) by using the NE2001 model of [Cordes & Lazio \(2002\)](#) which are consistent with each other. The most precisely measured proper motion is  $\mu_\alpha^* = -23.57^{+0.10}_{-0.10} \text{ mas yr}^{-1}$ ,  $\mu_\delta = 52.87^{+0.09}_{-0.10} \text{ mas yr}^{-1}$  corresponding to a transverse velocity of  $357^{+59}_{-43} \text{ km s}^{-1}$  at  $1.3^{+0.22}_{-0.16}$  kpc ([Chatterjee et al. 2009](#)). Although it presents no clear  $\gamma$ –ray emission ([Katsuta et al. 2012](#)), the pulsar is observable in soft X–rays due to thermal emission. PSR J0538+2817 is famous for being one of the few thermal pulsars: Based on a black-body model, the surface temperature and the emitting radius are given as  $T = 2.12 \times 10^6 \text{ K}$  and  $R = 1.68 \pm 0.05 \text{ km}$  ([McGowan](#)

**Table 2.** BVJHK (in mag) and pm (in  $\text{mas yr}^{-1}$ ) values of HD 37424.

Parameter	Value
B	$9.062 \pm 0.017$
V	$8.989 \pm 0.019$
J	$8.666 \pm 0.017$
H	$8.696 \pm 0.026$
K	$8.699 \pm 0.019$
$\mu_\alpha^*$	$10.8 \pm 0.8$
$\mu_\delta$	$-10.2 \pm 0.6$

[et al. 2003](#)). The hydrogen atmosphere model with  $B = 1 \times 10^{12}$  G gives  $T = 2.12 \times 10^6 \text{ K}$  and  $R \simeq 10 \text{ km}$  ([Zavlin & Pavlov 2004](#)). A faint pulsar wind nebula is observed in X–rays but not in radio ([Gaensler et al. 2000](#)). It is not known whether the observed elongated structure is the torus or the jets of the PWN. But assuming that it is due to the torus, it provides valuable information on the spin–kick alignment.

HD 37424 is a sound OB runaway star at 10.3 arcmin away from the GC to the west at  $\alpha = 05\text{h}39\text{m}44.4\text{s}$ ,  $\delta = +27^\circ 46'51.2''$ . Photometric and kinematic information on the star is given in Table 2. While proper motion values were retrieved from the UCAC4 catalog ([Zacharias et al. 2012](#)), the photometric magnitudes are obtained from the ASCC-2.5 V3 catalog ([Kharchenko 2001](#)). Its spectral type was previously identified as B0.5/1 IV/V ([Clausen & Jensen 1979](#)). As there was no public data nor a visualized spectrum, we established the spectral type again by taking a spectrum. The star has a very high proper motion compared to other early type and possibly distant stars. There is no reported variability or binarity in the literature. Hence, HD 37424 is a good OB runaway star candidate.

### 3 OBSERVATIONS

HD 37424 was observed at the TÜBİTAK National Observatory (TUG) with the TUG Faint Object Spectrograph and Camera (TFOSC) mounted on the 150 cm Russian Turkish Telescope (RTT-150). The observations were carried out on 2013 August 9 and 10. Two spectra were obtained with a 600 s exposure time for each. Grism 14 was used with a 67 micron slit. The wavelength range in this configuration is 3270–6120 Å and the resolving power ( $R$ ) is  $\sim 1337$ . 5 He lamp spectra taken in the same night with the object were used for wavelength calibration, and 5 halogen lamp spectra were obtained in the beginning and at the end of the night for flat-fielding. Also, 2 more targets had been observed in the same way on 2012 September 13 and 14 for the search for the runaway star. With the same purpose, 12 objects were observed at the Calar Alto Observatory on 2013 January 29 with Calar Alto Faint Object Spectrograph (CAFOS) on the 2.2 meter telescope. The covered wavelength range of the grism B-200 is 3200–7000 Å and  $R \sim 550$ . 3 HgCdAr and 3 halogen spectra were taken in the beginning and in the end of the night for wavelength calibration and flat-fielding. The high resolution observations of HD 37424 were performed at the Fred L. Whipple Observatory on 2013 September 16 and 21. The Tillinghast Reflector Echelle Spectrograph (TRES) mounted on the 1.5 meter telescope was used. Two spectra were taken at  $R \sim 44000$  in a broad wavelength range; 3800–9100 Å for 300 s exposure time. HD 36665 which is supposed to be a background object to the SNR was observed on 2014 February 11 with the Fibre Linked Echelle Astronomical Spectrograph (FLECHAS) (Mugrauer et al. 2014) at the University Observatory Jena. The covered wavelength range is 3900–8100 Å and  $R \sim 9200$ . Three spectra with 600 s exposure time were obtained. Three tungsten and 3 Th-Ar lamp spectra were taken immediately before this set for flat-fielding and wavelength calibration.

The observations of SNR S147 were performed at the University Observatory Jena with the Schmidt-Teleskop-Kamera (STK), operated in the Schmidt-focus of the 90 cm telescope of the observatory (see Mugrauer & Berthold (2010)). The observations were carried out with the narrow-band  $H\alpha$  filter of the STK, which spans a full-width-half-maximum of 5 nm. In total, 22 fields on the sky were observed during 5 nights, each with a field of view of  $52.8' \times 52.8'$ . At each position two 600 s integrations were taken with the STK, i.e. about 7.3 hours of integration time in total. The individual raw images per field were dark- and flatfield-corrected and finally averaged. Point sources detected in the overlap regions of the fully processed images were then used to create the mosaic image of SNR S147, shown in Figure 1, which covers a total field of view of  $4.8^\circ \times 4.1^\circ$ .

FLECHAS, TFOSC and CAFOS data were reduced with IRAF. All raw frames from TFOSC and CAFOS were over-scanned and no further subtraction was done as long as the over-scanned dark frames yields null count. Yet, FLECHAS images were subtracted by the dark frames taken in the previous night. The exposure time of a dark frame is the same as that of the corresponding science or calibration frame. Hence, the illumination effect was removed.

Then, the flat images were combined while rejecting the frames having minimum and maximum counts. Next, the object spectra were extracted by assigning an appropriate background region to each. The arc spectra were extracted as traced by the corresponding aperture of the object spectra. After wavelength calibration was performed, all spectra were normalized.

The final spectra were compared with MK standard star

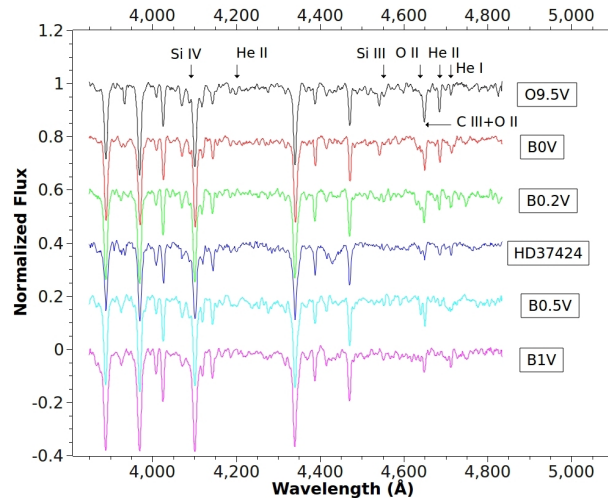


**Figure 2.** TFOSC spectrum of HD 37424 compared to main sequence B type stars. Distinctive features are marked. From left to right; Si IV  $\lambda 4089$ , He II  $\lambda 4200$ , Si III  $\lambda 4552$ , O II  $\lambda 4640$ , C III+O II  $\lambda 4650$  blend, He II  $\lambda 4686$ , He I  $\lambda 4713$

spectra retrieved from Walborn & Fitzpatrick (1990). To maintain equally resolved spectra, the standard spectra were boxcar smoothed by 13. Figure 2 shows the TFOSC spectrum of HD 37424 comparing with main sequence B type stars from various subclasses. HD 37424 shows He II  $\lambda 4686$  absorption indicating that the spectral type is earlier than B1. This feature is not seen in stars with a spectral type later than B0.7. On the other hand, He I lines (i.e. He I  $\lambda 4713$ ) are not as weak as in O type stars compared to He II lines;  $\lambda 4200$ ,  $\lambda 4686$ . The Si IV  $\lambda 4116$  line is totally blended and unmeasurable. Si III  $\lambda 4552$  is in low strength compared to Si IV  $\lambda 4089$  like in the B0V type spectrum. This ratio decreases towards higher temperatures, but He I  $\lambda 4541$  is not stronger than Si III  $\lambda 4552$  as seen in B0V and O9.5V spectra. Given the equal strengths of O II  $\lambda 4640$ , He II  $\lambda 4686$ , He I  $\lambda 4713$  and more intense C III+O II  $\lambda 4650$  blends, HD 37424 matches best with B0.2V. Considering the slightly stronger He I  $\lambda 4713$ , B0.5 would be the best approach to the temperature class of the star. Si IV  $\lambda 4089$  strength increases against He I  $\lambda 4026$ – $4144$  as the luminosity class goes higher. However, neutral helium lines are strong enough to judge that HD 37424 is a main sequence star; B0.5V. The spectral type is between B0.2V–B0.7V, but it is assumed as  $B0.5 \pm 0.5V$  in the distance and extinction calculations to avoid underestimation of the errors.

The sources observed by CAFOS are foreground stars with a maximum distance of  $671_{-56}^{+96}$  pc. Their spectral properties were identified by the same procedure as done for HD 37424. However, due to the lower resolution CAFOS spectra have higher uncertainty (Table 3). We used FLECHAS to identify the spectral types of the background star HD 36665. This is a  $B1 \pm 0.5V$  type star (Figure 3).

TRES data were used for radial velocity (RV) measurements of HD 37424. Due to the low signal to noise, 10 absorption features could be used (Table 4). Doublets or triplet lines are avoided as these features increased the dispersion significantly. The lines were fitted by Gaussian functions and the best shifts were determined. Two more Gaussian fits with different centers were applied for each line; one fits the outer edge of the noise of the blue side while fitting the inner edge of the red. The other fits the outer edge of the red and the inner edge of the blue. By doing this, underesti-

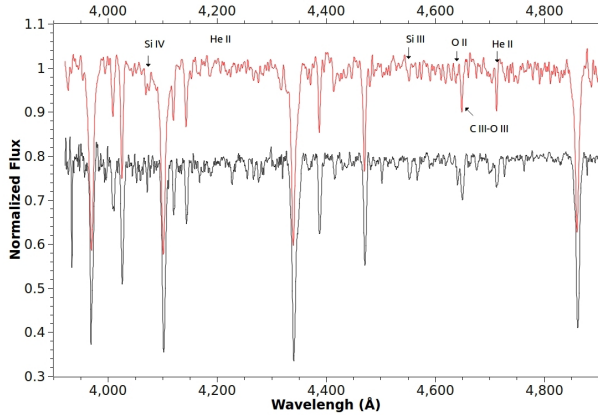


**Figure 3.** The FLECHAS spectrum of HD 36665 (black) in comparison with a B1V template.

**Table 3.** Observed stars in the region. Names, angular separations to the SNR GC (in arcmin), spectral types, instruments used and distances with upper and lower errors (in pc) are given. The error in temperature subclasses is  $\pm 1$  for those with integer value and  $\pm 0.5$  for those with half integer value. The resolution of CAFOS is not enough to distinguish the luminosity classes IV and V. Yet, the stars are assumed to be in luminosity class V.

Name	Angular Separation	Spec. Type	Inst. <sup>1</sup>	Distance	Distance (Error)
TYC 1869-01281-1	19.4	A2V	C	574	+73 / -41
TYC 1869-01317-1	5.5	B9.5V	T	1013	+183 / -174
TYC 1869-01334-1	25.5	F2V	C	289	+38 / -34
TYC 1869-01376-1	27.9	A7V	C	428	+18 / -32
TYC 1869-01505-1	23.5	F1V	C	380	+50 / -44
TYC 1869-01610-1	17.6	F7V	C	245	+18 / -16
TYC 1869-01632-1	27.2	F8V	C	316	+37 / -26
TYC 1869-01642-1	5.61	B9.5V	T	952	+172 / -163
TYC 1869-01679-1	25.6	G2V	C	170	+11 / -9
TYC 1869-01749-1	20.1	F8V	C	166	+19 / -14
TYC 1873-00145-1	25.0	A3V	C	603	+46 / -50
TYC 1873-00307-1	29.2	F8V	C	326	+40 / -29
TYC 1873-00347-1	19.8	A0V	C	671	+96 / -56
UCAC4-589-020390	22.1	F4V	C	381	+14 / -16

<sup>1</sup> Instruments: C: CAFOS, T: TFOSC

matting the errors is avoided. As the features are wide and the data are noisy, the centers of these secondary fits are far away from the best fits,  $16 \text{ km s}^{-1}$  on average. The difference between the best fit and the upper limit (towards red) fit is distinct from the best fit and the lower limit (towards blue) difference. To avoid underestimating the error, the greater difference is assigned as the final error. The average heliocentric velocities of the first and the second spectra are  $-9.2$  and  $-9.1 \text{ km s}^{-1}$  with line to line scattering standard deviations being  $6.5$  and  $5.5 \text{ km s}^{-1}$  respectively.

As long as the star is inside the supernova remnant, high velocity gas accelerated by the SNR is expected to reveal itself as blue-shifted components to Ca II–K and H and/or Na I–D1 and D2 absorption features. The spectra show no clear high velocity features (Figure 4). The average heliocentric velocity of the interstellar gas is  $12.1 \pm 0.5 \text{ km s}^{-1}$  (Table 5). This is typical for the neighboring stars (Silk & Wallerstein 1973). The star has no positional correspondence with bright filaments, but with fainter H $\alpha$  emitting regions. It is located at the vicinity of the eastern cavity seen in the

**Table 4.** Radial velocity measurements of HD 37424. The laboratory wavelength of the features, the Gaussian width ( $\sigma$ ) of the fit, the wavelength shift obtained by the best fitting Gaussian, upper and lower limits of the shift from different Gaussian fits and the final error are presented. The features are given in Å while all other columns are in  $\text{km s}^{-1}$

Feature	$\sigma$	Observations on September 16th, 2013			
		BF	UL	LL	E
3889.051	164	-10.1	19.3	-29.2	29.4
3970.074	137	-0.5	21.4	-22.3	21.9
4101.737	144	-9.4	12.2	-32.3	22.9
4143.759	98	+4.0	17.1	-10.9	14.9
4340.468	142	-10.6	6.2	-28.8	18.2
4387.928	81	-13.1	-7.1	-24.1	11
4861.332	139	-13.8	0.9	-18.9	14.7
4921.929	89	-16.5	-1.6	-32.4	15.9
6562.817	115	-14.7	0.3	-21.5	15
6678.149	82	-7.5	0.3	-14.5	7.8
Feature	$\sigma$	Observations on September 21st, 2013			
		BF	UL	LL	E
3889.051	164	-12.6	6.2	-28.2	18.8
3970.074	137	-1.4	18.0	-19.8	19.4
4101.737	144	-5.1	14.9	-21.2	20
4143.759	98	-1.9	7.2	-8.7	9.1
4340.468	142	-11.5	11.9	-36.6	25.1
4387.928	81	-8.8	-4.1	-19.3	10.5
4861.332	139	-11.7	-3.0	-19.5	8.7
4921.929	89	-17.2	-4.9	-31.6	14.4
6562.817	115	-14.4	1.4	-29.7	15.8
6678.149	82	-6.7	3.3	-15.1	10

BF: Best fit, UL: Upper Limit, LL: Lower Limit, E: Error

**Table 5.** Measured velocities for interstellar Ca II–K and H and Na I–D1 and D2 lines. These lines have a low Gaussian width unlike the intrinsic features of the star. The average velocity is  $12.1 \text{ km s}^{-1}$  with a standard deviation  $0.5 \text{ km s}^{-1}$  in each observation. The data in the first column are in (Å) while the others are in  $\text{km s}^{-1}$ .

Feature	$\sigma$	Velocity (Day 1)	Velocity (Day 2)
3933.664	7.5	12.3	11.8
3968.47	5.9	12.8	12.7
5889.953	9.0	11.6	11.6
5895.923	8.3	11.9	12.0

Day 1: Sep. 16th, 2013; Day 2: Sep 21st, 2013.

radio and  $\gamma$ -ray images (Kundu et al. 1980; Katsuta et al. 2012). As the star can hardly be a foreground source, we suggest that, in this direction, the shocked ejecta has not reached the dense interstellar gas yet. The reader must note that, the background stars displaying high velocity Ca II lines in Sallmen & Welsh (2004) are located behind bright filament knots. The high velocity gas is found where the filaments are concentrated (Lozinskaya 1976).

Using the absolute visual magnitude from Aller et al. (1982), for a spectral type  $B0.5V \pm 0.5$ , the distance modulus yields  $1868^{+410}_{-403} \text{ pc}$  for HD 37424. Using the luminosity of the same spectral type from Hohle et al. (2010), we find the distance as  $1318 \pm 119 \text{ pc}$  which is well consistent with the distance of the pulsar. The total visual absorption was taken into account in both calculations.

As the absolute magnitudes for early type stars can range from

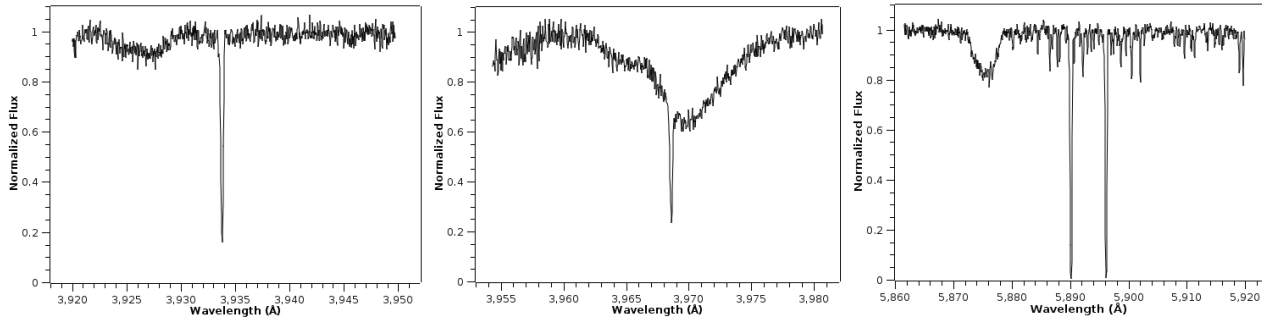


**Figure 4.** The strong interstellar lines of HD37424. *Left:* Ca II–K line from TRES spectrum. Despite a weak blended feature at  $-13 \text{ km s}^{-1}$ , there is no clear high velocity component. *Middle:* Ca II–H line (He I as a background) from the same spectrum. Again there is no clear high velocity gas component. *Right:* Interstellar Na I–D1 and D2 lines. The feature with high FWHM is the He I  $\lambda 5875$  triplet. Those around Sodium doublet are tellurics.

star to star in the same temperature, interstellar Ca II lines are also used in distance determination. By using the following relation from Megier et al. (2009),

$$D = 77 + \left( 2.78 + \frac{2.60}{\frac{EW(K)}{EW(H)} - 0.932} \right) EW(H) \quad (1)$$

the distance to HD 37424 is found to be  $1288^{+304}_{-193}$  pc which is almost in the same range as the pulsar. The equivalent widths are  $243 \pm 7$  and  $160 \pm 15 \text{ m}\text{\AA}$  for Ca II–K and Ca II–H lines respectively.

The extinction towards the star was also derived from 4430 and 4502 Å DIB’s. The measured equivalent widths have high error due to the blending. Using the EW’s, the E(B–V) was calculated based on the relation mentioned in Herbig (1975). It yields  $0.42 \pm 0.08$  mag; points to somewhat larger color excess but does not exclude  $0.35 \pm 0.04$  mag derived from photometry.

#### 4 KINEMATICS

HD 37424 and PSR J0538+2817 have proper motions receding from each other and departing from the same location on the sky (Figure 1). The proper motion of both objects are corrected for Galactic rotation and solar motion. The Galactocentric distance to the Sun is taken as 8.5 kpc and the solar rotational velocity as  $220 \text{ km s}^{-1}$ . The local standard of rest was taken from Tetzlaff et al. (2011) as  $(U_{\odot}, V_{\odot}, W_{\odot}) = (10.4 \pm 0.4, 11.6 \pm 0.2, 6.1 \pm 0.2) \text{ km s}^{-1}$ . The resultant values for HD 37424 are  $\mu_{\alpha}^* = 10.0 \pm 0.8 \text{ mas yr}^{-1}$ ,  $\mu_{\delta} = -5.9 \pm 0.6 \text{ mas yr}^{-1}$  and for the pulsar,  $\mu_{\alpha}^* = -24.4 \pm 0.1 \text{ mas yr}^{-1}$ ,  $\mu_{\delta} = 57.2 \pm 0.1 \text{ mas yr}^{-1}$ . Together with the  $-20.0 \pm 6.5 \text{ km s}^{-1}$  peculiar radial velocity, HD 37424 has a space velocity of  $74 \pm 8 \text{ km s}^{-1}$  at 1.3 kpc. HD 37424 is a runaway star of which velocity is higher than typical runaway velocities 40–50  $\text{km s}^{-1}$ . The 2–D space velocity of the pulsar at the same distance is  $382.2 \pm 0.8 \text{ km s}^{-1}$ .

We constructed the past 3D trajectories of PSR J0538+2817 and the runaway star HD 37424 to evaluate whether these two objects could have been at the same place at the same time in the past. Since we applied the same method already in preceding papers (Tetzlaff et al. 2010, 2011, 2012), we refer to these publications for details. We construct three million past trajectories of PSR J0538+2817 and HD 37424 throughout Monte Carlo simulations by varying the observables (parallax, proper motion, radial velocity) within their error intervals. For the radial velocity of the NS, we assume a uniform distribution in the range of  $-1500$  to  $+1500 \text{ km s}^{-1}$ . From all pairs of trajectories, we evaluate the smallest sep-

aration  $d_{min}$  and the past time  $\tau$  at which it occurred. The distribution of separations  $d_{min}$  is supposed to obey the distribution of absolute differences of two 3D Gaussians (see e. g. Hoogerwerf et al. 2001, equations A3 and A4; Tetzlaff et al. 2012, equations 1 and 2), if it is assumed that the stellar 3D positions are Gaussian distributed. Since the actual (observed) case is different from this simple model (no 3D Gaussian distributed positions, due to e. g. the Gaussian distributed parallax that goes into the position reciprocity, uniform radial velocity distribution of the NS, etc.), we adapt the theoretical formulae (we use equations 1 and 2 in Tetzlaff et al. (2012) with the symbols  $\mu$  and  $\sigma$  for the expectation value and standard deviation, respectively) only to the first part of the  $d_{min}$  distribution (up to the peak plus a few more bins, see Tetzlaff et al. 2012). The derived parameter  $\mu$  then gives the positional difference between the two objects.<sup>1</sup>

We find that both stars were at the same position in the past i.e.  $\mu = 0$  at  $(l, b) = (84.82 \pm 0.01, 27.84 \pm 0.01) \text{ deg}$  at  $30 \pm 4 \text{ kpc}$  (Figure 5). This predicted position of the supernova is  $4.2^{+0.8}_{-0.6}$  arcmin offset from the nominal geometric center. The predicted distance of the supernova (as it is seen from the Earth today) is  $1333^{+103}_{-112} \text{ pc}$ .

#### 5 ASSOCIATIONS

There is no known OB association within  $4.5^{\circ}$  ( $\sim 100 \text{ pc}$  at 1300 pc) from SNR S147. Considering the angular separations and radial distances, the progenitor star cannot be linked to any of the young open cluster around. Hence, it is considered to be a runaway star ejected e.g. from the cluster NGC 1960, which is 217 pc away from the SNR, several millions years ago (Ng et al. 2007). However, binarity among cluster ejected runaway stars are rare (Gies & Bolton 1986). So, as the progenitor was the previous binary companion to HD 37424, it may be unlikely that they were ejected from a cluster. Therefore, the neighboring stars are investigated to search for any association. All of the OB type stars within  $4.5^{\circ}$  (100 pc at 1.3

<sup>1</sup> The uncertainties on the separation are dominated by the kinematic uncertainties of the NS that are typically of the order of a few hundred  $\text{km s}^{-1}$  (because of the assumed radial velocity distribution). As a consequence, the distribution of separations  $d_{min}$  shows a large tail for larger separations. However, the first part of the  $d_{min}$  distribution (slope and peak) can still be explained well with the theoretical curve (here equation 2 in Tetzlaff et al. 2012) since the kinematic dispersion for only those runs are much smaller, a few tens of  $\text{km s}^{-1}$  for the NS, i.e. a few tens of pc after 1 Myr.

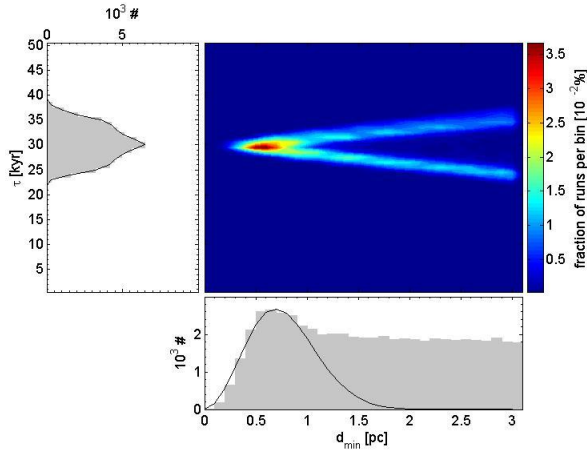


**Figure 5.** Distributions of minimum separations  $d_{min}$  and corresponding flight times  $\tau$  for encounters between PSR J0538+2817 and HD 37424. The solid curves drawn in the  $d_{min}$  histogram (bottom panel) represent the theoretically expected distribution with  $\mu = 0$  and  $\sigma = 0.35$  pc, adapted to the first part of the histogram.

kpc distance) of the geometrical center (GC) of the SNR were selected from *The Catalogue of Stellar Spectral Classifications* (Skiff 2013). The spectral types are known through spectroscopic observations. There are some discrepancies in spectral types reported by different papers. So, always the latest reference was chosen. Together with 14 stars from our observations at TUG and Calar Alto, 99 stars are used. The photometric data were obtained from the catalog *ASCC-2.5 V3* (Kharchenko 2001) except for UCAC4–589–020390 of which photometric data was retrieved from the *UCAC4* catalog.

For each star having an integer spectral subclass, distance and extinction are calculated in an interval between one spectral subclass above and below, e.g. B0V–B2V for a B1V type star. For those having half integer subclass, half spectral subclass above and below are used e.g. B0V–B1V for a B0.5V type star. The total visual extinction,  $A_V$ , was determined by using BVJHK colors and intrinsic color differences of corresponding spectral types. Using the following relation,  $A_V$  values were derived for each color difference; B–J, B–H, B–K, V–J, V–H, V–K.

$$A_V = \frac{(\lambda_1 - \lambda_2) - (\lambda_1 - \lambda_2)_0}{A_{\lambda_1}/A_V - A_{\lambda_2}/A_V}, \quad (2)$$

The intrinsic colors are obtained from Kenyon & Hartmann (1995) and Wegner (1994), while  $A_\lambda/A_V$  ratios are from Rieke & Lebofsky (1985). Color differences of short intervals, i.e. H–K have high errors as they are multiplied by higher coefficients. The color excess  $E(B-V)$  is mentioned separately. (Table 6)  $A_V$  values obtained from six color differences were averaged and their standard deviation were calculated. This was applied for all three possible spectral types of the source. As long as the error due to the spectral type uncertainty is larger than the standard deviation of the color differences, it was assigned to be the final error. When the error is asymmetric due to the intrinsic colors of different spectral types, the larger one was accepted. In some cases, the uncertainty is dominated by the error in color differences. Then, these were preferred to be the final error for such sources.  $E(B-V)$  versus  $A_V$  fit yields a total to selective absorption ratio is  $3.24 \pm 0.06$ . In individual cases,  $E(B-V)$  deviates strongly from  $A_V$ . However, the large sample reveals that the ratio of total to selective absorption has a usual value. The distances were derived from distance moduli using the absolute

**Table 7.** Visual absolute magnitudes at  $1.3 \pm 0.1$  kpc for the stars of the possible OB association of which HD 37424 is a member. Errors are mainly due to the distance range 1.2–1.4 kpc. The expected  $M_V$  for the corresponding spectral types and its dispersion from Wegner (2006) (W06) are given. All values are in mag.

Name	$M_V$ (@ 1.3±0.1 kpc)	error	$M_V$ (W06)	Disp. (W06)
TYC 1869-01317-1	-0.14	+0.26 / -0.27	+0.29	1.40
TYC 1869-01642-1	-0.28	+0.26 / -0.27	+0.29	1.40
HD 37424	-2.86	+0.22 / -0.23	-3.34	2.40
HD 36993	-3.67	+0.22 / -0.23	-4.02	2.30
HD 37318	-4.46	+0.31 / -0.32	-3.34	2.40
BD+27 797	-2.97	+0.30 / -0.31	-3.34	2.40
HD 37696	-3.72	+0.22 / -0.23	-3.34	2.40
BD+27 850	-2.52	+0.20 / -0.21	-2.95	1.16
HD 245770	-3.49	+0.29 / -0.30	-3.34	2.40
HD 36441	-3.46	+0.29 / -0.30	-2.95	1.16
BD+26 943	-2.36	+0.30 / -0.31	-2.64	1.40
HD 38010	-5.04	+0.26 / -0.27	-4.10	2.20
BD+30 938	-2.95	+0.20 / -0.21	-2.32	1.50
Sh 2-242 1	-2.74	+0.29 / -0.30	-3.34	2.40
HD 37366	-4.15	+0.22 / -0.23	-4.49	2.27
BD+30 987	-1.86	+0.24 / -0.25	-1.49	2.00
BD+30 976	-1.18	+0.33 / -0.34	-0.63	1.40
BD+25 989	-2.41	+0.29 / -0.30	-2.95	1.16
BD+27 909	-2.96	+0.26 / -0.27	-2.63	2.20
BD+31 1065	-1.76	+0.20 / -0.21	-2.32	1.50
BD+31 1050	-2.30	+0.19 / -0.20	-2.32	1.50
HD 38909	-2.98	+0.19 / -0.20	-2.32	1.50
BD+31 1021	-1.15	+0.28 / -0.29	-0.63	1.40
HD 40297	-4.37	+0.29 / -0.30	-3.75	1.30

magnitudes from Aller et al. (1982). Errors in distances are due to the uncertainty in spectral type and the error in  $A_V$  were also taken into account.

The spectro–photometric distance alone is not enough due to the high dispersion in the brightness of OB–type stars (Wegner 2006) (Thereafter W06). Assuming the stars beyond 1 kpc are within 100 pc from the SNR GC, the absolute visual magnitudes were calculated. Although the dispersion mentioned in W06 is high, 24 of the stars fit well in the comparison with the W06 values. Hence, we suggest that these stars are members of an OB association. (Table 6, Table 7, 19 of them have similar pm values. The average pm in right ascension is  $-1.39 \text{ mas yr}^{-1}$  and  $-4.17 \text{ mas yr}^{-1}$  in declination with  $0.99 \text{ mas yr}^{-1}$  and  $1.45 \text{ mas yr}^{-1}$  standard deviation respectively (Table 8). At 1.3 kpc, 5 of them are runaway stars exceeding  $20 \text{ km s}^{-1}$ –D peculiar velocity. This is consistent with the general ratio of the runaway stars to the normal stars which is 10–30 percent (Gies 1987).

## 6 DISCUSSION

The runaway nature of HD 37424 is clear. The chance projection of such a massive runaway star moving away from the GC of an SNR in the Galactic anti–center direction must be very low. In addition, combining with the central compact object after tracing back both objects at the same time shows that HD 37424 is clearly the pre–supernova binary companion of the progenitor of SNR S147 and PSR J0538+2817. BSS is the favored explanation for its runaway nature.

HD 37424 is a B0.5V type star with a mass of  $\sim 13 M_\odot$  (Hohle et al. 2010). So, the progenitor of the pulsar must have a

**Table 6.** 24 stars beyond 1 kpc are presented. Angular distances are given in degrees, distances in parsecs, extinctions and brightness in visual band in magnitudes. In the column; SpT adopted, the average spectral types that are used in distance calibrations are given.

Ang. Sep.	Name	SpT	SpT (adopted)	$A_V$	$A_V$ (Err)	E(B-V)	E(B-V) (Err)	Distance	Distance (Err)	V	Ref#*
0.09	TYC 1869-01317-1	B9.5V	B9.5V	0.83	0.1	0.26	0.090	1013	+183 / -174	11.258	tw
0.09	TYC 1869-01642-1	B9.5V	B9.5V	1.00	0.1	0.3	0.090	952	+172 / -163	11.293	tw
0.17	HD 37424	B0.5V	B0.5V	1.28	0.06	0.35	0.036	1868	+410 / -403	8.989	tw
0.52	HD 36993	B0.5/III/IV	B0.5III-IV	1.35	0.06	0.39	0.028	1961	+636 / -628	8.248	1
0.63	HD 37318	B0.5Ve	B0.5V	2.29	0.15	0.59	0.026	903	+231 / -228	8.399	1
1.00	BD+27 797	B0.5Ve	B0.5V	2.50	0.14	0.62	0.094	1788	+485 / -465	10.095	2
1.35	HD 37696	B0.5IV/V	B0.5IV-V	1.12	0.06	0.29	0.023	1549	+565 / -558	7.973	1
1.35	BD+27 850	B1.5IVe	B1.5V	1.31	0.04	0.35	0.056	1525	+313 / -305	9.362	2
1.52	HD 245770	O9/B0III/Ve	B0III-V	2.11	0.13	0.79	0.053	2595	+1090 / -1066	9.187	3
1.76	HD 36441	B0.5/1.5V	B1V	1.13	0.13	0.33	0.058	1153	+628 / -389	8.239	1
1.97	BD+26 943	B2V	B1.5V	1.41	0.14	0.37	0.040	1357	+723 / -511	9.623	8
2.61	HD 38010	B1III	B1III	1.29	0.1	0.22	0.028	967	+437 / -236	6.817	4
2.95	BD+30 938	B3III	B3III	1.44	0.04	0.45	0.030	1332	+741 / -255	9.062	7
2.98	Sh 2-242 1	B0V	B0V	2.17	0.13	0.78	0.056	2318	+853 / -842	9.996	5
3.06	HD 37366	O9.5V	O9.5V	1.22	0.06	0.35	0.016	1375	+201 / -199	7.640	6
3.07	BD+30 987	B5III:	B5III	0.73	0.08	0.25	0.044	1523	+398 / -287	9.444	7
3.24	BD+30 976	B7V	B7V	0.89	0.17	0.18	0.020	994	+264 / -226	10.277	7
3.45	BD+25 989	B1Vn	B1V	1.59	0.13	0.43	0.082	1872	+1061 / -649	9.751	8
3.61	BD+27 909	B2III	B2III	1.87	0.1	0.55	0.076	2004	+683 / -761	9.479	8
4.05	BD+31 1065	B3III	B3III	0.67	0.04	0.27	0.043	2304	+1286 / -442	9.482	7
4.07	BD+31 1050	B3III	B3III	1.01	0.03	0.35	0.047	1791	+988 / -338	9.276	7
4.09	HD 38909	B3II-III	B3II-III	0.56	0.03	0.17	0.033	2057	+1007 / -992	8.145	9
4.28	BD+31 1021	B7V	B7V	1.05	0.12	0.14	0.106	1007	+250 / -218	10.465	7
4.46	HD 40297	B9.5Ib/II	B9.5Ib/II	1.07	0.13	0.25	0.015	1337	+693 / -688	7.270	1

\* Ref#: 1: [Clausen & Jensen \(1979\)](#); 2: [Steele et al. \(1999\)](#); 3: [Wang & Gies \(1998\)](#); 4: [Cucchiaro et al. \(1976\)](#); 5: [Hunter & Massey \(1990\)](#); 6: [Walborn \(1971\)](#); 7: [Bouigue et al. \(1961\)](#); 8: [Christy \(1977\)](#); 9: [Morgan et al. \(1955\)](#); 10: [Christy \(1977\)](#); tw: This work.

**Table 8.** 19 stars with common proper motion are presented. The average  $PM_{RA}$  is  $-1.39$  mas  $yr^{-1}$  and  $PM_{Dec}$  is  $-4.17$  mas  $yr^{-1}$ . The last three column represents the 2-D space velocity of the stars with respect to the average motion of the group with maximum and minimum values in  $km s^{-1}$ . All the values of proper motions are in  $mas yr^{-1}$ .

Name	$\mu_{\alpha}^*$	err	$\mu_{\delta}$	err	$V_{REL}$	max	min
HD 37318	-0.8	0.6	-5.9	0.6	11.2	16.1	6.9
TYC 1869-01642-1	-1.5	1.1	-2.4	1.2	11.0	19.8	7.1
HD 38010	-1.7	1.0	-3.3	1.0	5.7	14.1	0.0
BD+30 976	-3.5	0.9	-5.3	0.5	14.7	21.1	8.4
BD+31 1021	-2.8	0.7	-5.5	0.8	11.9	18.4	5.4
TYC 1869-01317-1	-0.9	0.9	-5.1	0.9	6.5	14.2	0.0
HD 36441	-2.0	0.6	-6.6	0.6	15.4	20.1	11.2
BD+30 938	-1.7	0.8	-3.6	0.6	4.0	9.9	0.0
HD 40297	-1.4	1.0	-3.7	1.0	2.9	11.0	0.0
BD+26 943	-0.9	0.8	-3.7	0.8	4.2	11.2	0.0
BD+30 987	-2.0	0.6	-4.7	1.2	4.9	13.0	0.0
BD+27 797	-0.1	0.7	-3.1	1.4	10.4	19.6	4.2
BD+31 1050	-1.0	0.6	-4.0	0.6	2.7	7.8	0.0
BD+25 989	-1.5	0.9	-2.5	1.6	10.3	21.1	4.9
HD 36993	-0.2	0.9	-5.8	0.6	12.4	18.8	6.6
HD 38909	+0.7	0.5	-4.2	1.5	12.9	18.4	0.0
BD+31 1065	-1.0	0.6	-1.3	0.5	17.9	21.7	14.7
Sh 2-242 1	-0.1	0.7	-1.8	1.0	16.7	24.2	9.2
HD 245770	-2.0	0.5	-4.3	1.1	3.8	10.2	0.0

higher mass. Based on the lack of O type stars in the field (see Table 6) we set an upper mass limit of  $20\text{--}25 M_{\odot}$ . It may even imply a twin binary. The Roche Lobe radii calculated for 15, 20 and 25  $M_{\odot}$  vary between 91 and 311  $R_{\odot}$  which shows that the system

might have been an interacting binary. Hence, the progenitor star should be a naked helium star at the final stage of its evolution with a mass even as low as  $2 M_{\odot}$  ([van den Heuvel 1993](#)), ([Woosley et al. 1995](#)). However, how conservative the mass transfer was, will be understood after further observations. Assuming a circular orbit, pre-supernova binary parameters are calculated for 2, 5, 10, 15, 20 and 25  $M_{\odot}$  (Table 9) progenitor masses.

As discussed in the previous section, the OB stars around might be members of an unidentified old OB association of which all of the O type stars underwent supernova explosions. This also makes a plausible explanation for the low density medium in which the SNR expands symmetrically. But, an ejection of the pre-SN system is also possible. A membership to an OB association or to a cluster is important also regarding the distance determination. In this work, the distance derived from pulsar parallax ( $1.3_{-0.16}^{+0.20}$  kpc) is accepted as the most reliable estimation. Also, the distance to the star measured from interstellar lines is in the same range,  $1288_{-193}^{+304}$  pc (see section 3). The spectro-photometric distance is much larger by using absolute magnitudes from [Aller et al. \(1982\)](#). Yet, by using typical luminosities for B0.5V type suggested in [Hohle et al. \(2010\)](#), it is  $1318 \pm 119$  pc. Hence, the distance to the star and the SNR can be assumed to be 1.3 kpc. However, the  $A_V$  measured directly towards S147 is much lower than the  $A_V$  towards the stars beyond 1 kpc. Furthermore, two stars, HD 36665 and HD 37318, show highly shifted interstellar Ca II and Na I lines related to the SNR implying that these objects are background sources ([Sallmen & Welsh 2004](#)). Their distances based on the reported spectral types are closer to the Sun than HD 37424 is. HD 36665 has  $837_{-285}^{+347}$  pc for B1V type and HD 37318 is  $903_{-228}^{+231}$  pc far away adopting B0.5V. On the other hand, the distance for HD 36665 is identified as 1860 pc in [Neckel et al. \(1980\)](#) through  $H_{\beta}$  measurements. It

**Table 9.** The binary separations, the orbital velocities of the progenitor, the orbital periods and the Roche Lobe radii of the pre-supernova binary for various final masses of the progenitor with  $13 M_{\odot}$  HD 37424 are given. Roche Lobe radii are calculated based on Eggleton (1983).

Progenitor Mass ( $M_{\odot}$ )	2	5	10	15	20	25
Binary Separation ( $R_{\odot}$ )	$9_{-3}^{-1}$	$49_{+11}^{-9}$	$152_{+37}^{-26}$	$281_{+68}^{-49}$	$425_{+101}^{-75}$	$576_{+137}^{-101}$
Orbital Velocity ( $\text{km s}^{-1}$ )	$481 \pm 49$	$192 \pm 20$	$96 \pm 10$	$64 \pm 7$	$48 \pm 5$	$38 \pm 4$
Orbital Period (days)	$0.85_{+0.32}^{-0.22}$	$9_{+4}^{-2}$	$45_{+17}^{-11}$	$103_{+39}^{-26}$	$176_{+66}^{-44}$	$259_{+98}^{-65}$
Roche Lobe Radius ( $R_{\odot}$ )				$110_{+27}^{-19}$	$177_{+42}^{-31}$	$251_{+60}^{-44}$

has a high  $A_V$  of 1.74 mag. If we assume that HD 36665 is also at  $1.3 \pm 0.1$  kpc, then it must be a bright B1V type star which is 1–1.5 mag brighter than the average value given in W06. HD 37318 also can be a member of the possible OB association.

The supernova event had occurred quite nearby in a fairly reddened medium. Assuming a very faint SN ( $M_V = -14$  mag), the apparent visual magnitude is  $-2.1$  mag, and for a bright SN with  $M_V = -21$  mag, the apparent visual magnitude is  $-9.1$  mag; as bright as SN 1006. The event might have also caused the  $^{10}\text{Be}$  peak at  $35 \pm 2$  kyr measured in Raisbeck et al. (1987) from the deep ice cores from Dome C and Vostok Antarctica.

## 7 CONCLUSION

HD 37424 is a B0.5V type runaway star from a binary ejection due to the supernova which gave birth to SNR S147 and PSR J0538+2817. The star has  $-9.2 \pm 6.5 \text{ km s}^{-1}$  heliocentric radial velocity and  $74 \pm 8 \text{ km s}^{-1}$  3-D peculiar velocity. The distance calculated from interstellar Ca II lines is  $1288_{-193}^{+304}$  pc and from spectro-photometry  $1318 \pm 119$  pc. No high velocity gas related with the SNR is detected in the spectra. The past trajectories of the pulsar and HD 37424 are reconstructed throughout Monte Carlo simulations. It is found that both stars were at the same position at  $(l, b) = (84.82 \pm 0.01, 27.84 \pm 0.01)$  deg at  $30 \pm 4$  kyr in the past. The position of the explosion is  $4.2_{-0.6}^{+0.8}$  arcmin away from the geometrical center. The distance of the SNR is found as  $1333_{-112}^{+103}$  pc.  $A_V$  towards the SNR is  $1.28 \pm 0.06$  mag.

Today's kinematics of the stars are well known, further detailed calculations should be done to find the true kick vectors of the pulsar and a possible spin-kick alignment.

There is no known OB association reported close to the SNR. 19 OB type stars within 100 pc from the SNR geometrical center have very similar 2-D velocities with the 5 runaway stars including HD 37424. This might be an old OB association having no bright O type stars. The low density medium in which the SNR is expanding is probably due to the previous SNe and H II regions driven by this old association. The progenitor was a massive star with a zero age main sequence mass greater than  $13 M_{\odot}$ . Considering the lack of O type stars in the field, a progenitor mass much larger than  $20 M_{\odot}$  is not expected. Assuming a circular orbit, the pre-supernova binary separation is in the range of 8 to  $711 R_{\odot}$  for 2 to  $25 M_{\odot}$  final mass of the progenitor. The corresponding Roche Lobe radii for 15 to  $25 M_{\odot}$  masses vary from 91 to  $311 R_{\odot}$ . It must have been an interacting binary.

For 1.3 kpc distance and 1.3 mag extinction, the SN which happened  $30 \pm 4$  kyr ago had an apparent brightness of  $-2.1$  to  $-9.1$  mag.

The source will be investigated regarding the elemental signatures of binary accretion and the possible supernova debris on its photosphere through high resolution and high S/N spectra.

## ACKNOWLEDGEMENTS

This work was conceived by the late Oktay H. GUSEINOV (1938–2009). The authors acknowledge the leading role he had in all stages of this work and other related topics. His contribution to Galactic Astrophysics and his scholarship will be greatly missed. We thank Janos Schmidt and Christian Ginski for their observational support and Ronny Errmann for useful discussions. BD, NT and RN acknowledge support from DFG in the SFB/TR-7 Gravitational Wave Astronomy. This research has made use of Aladin. We would like to thank the Calar Alto observatory staff for their help in our observations; and we would like to thank DFG in NE 515 / 53-1 for financial support for the Calar Alto observing run. We also thank TÜBITAK National Observatory for their supports in using RTT-150 with project number 12ARTT150-267.

## References

- Allakhverdiev A. O., Guseinov O. H., Tagieva S. O., Yusifov I. M., 1997, *Astronomy Reports*, 41, 257
- Aller L. H. et al., eds, 1982, *Landolt-Börnstein: Numerical Data and Functional Relationships in Science and Technology - New Series "Gruppe/Group 6 Astronomy and Astrophysics" Volume 2 Schaifers/Voigt: Astronomy and Astrophysics / Astronomie und Astrophysik "Stars and Star Clusters / Sterne und Sternhaufen*
- Anderson S. B., Cadwell B. J., Jacoby B. A., Wolszczan A., Foster R. S., Kramer M., 1996, *ApJ*, 468, L55
- Ankay A., Kaper L., de Bruijne J. H. J., Dewi J., Hoogerwerf R., Savonije G. J., 2001, *A&A*, 370, 170
- Blaauw A., 1961, *Bull. of Astro. Inst. of the Netherlands*, 15, 265
- Bobylev V. V., 2008, *Astronomy Letters*, 34, 686
- Bouigue R., Boulon J., Pedoussaut A., 1961, *Annales de l'Observatoire Astron. et Meteo. de Toulouse*, 28, 33
- Chatterjee S. et al., 2009, *ApJ*, 698, 250
- Chevalier R. A., 1974, *ApJ*, 188, 501
- Christy J. W., 1977, *ApJ*, 217, 127
- Clark D. H., Caswell J. L., 1976, *MNRAS*, 174, 267
- Clausen J. V., Jensen K. S., 1979, in McCarthy M. F., Philip A. G. D., Coyne G. V., eds, *Ricerche Astronomiche Vol. 9, IAU Colloq. 47: Spectral Classification of the Future*. p. 479
- Cordes J. M., Lazio T. J. W., 2002, *ArXiv Astrophysics e-prints*
- Cucchiari A., Jaschek M., Jaschek C., Macau-Hercot D., 1976, *A&AS*, 26, 241
- Eggleton P. P., 1983, *ApJ*, 268, 368
- Feast M. W., Shuttleworth M., 1965, *MNRAS*, 130, 245
- Fesen R. A., Blair W. P., Kirshner R. P., 1985, *ApJ*, 292, 29
- Fuerst E., Reich W., 1986, *A&A*, 163, 185
- Gaensler B. M., Stappers B. W., Frail D. A., Moffett D. A., Johnston S., Chatterjee S., 2000, *MNRAS*, 318, 58

- Gies D. R., 1987, *ApJS*, 64, 545
- Gies D. R., Bolton C. T., 1986, *ApJS*, 61, 419
- Green D. A., 2009, *VizieR Online Data Catalog*, 7253, 0
- Guseinov O. H., Ankaý A., Sezer A., Tagieva S. O., 2003, *Astronomical and Astrophysical Transactions*, 22, 273
- Guseinov O. H., Ankaý A., Tagieva S. O., 2003, *Serbian Astronomical Journal*, 167, 93
- Guseinov O. H., Ankaý A., Tagieva S. O., 2004a, *Serbian Astronomical Journal*, 168, 55
- Guseinov O. H., Ankaý A., Tagieva S. O., 2004b, *Serbian Astronomical Journal*, 169, 65
- Guseinov O. H., Ankaý A., Tagieva S. O., 2004c, *International Journal of Modern Physics D*, 13, 1805
- Guseinov O. H., Ankaý A., Tagieva S. O., 2005, *Astrophysics*, 48, 330
- Hansen B. M. S., Phinney E. S., 1997, *MNRAS*, 291, 569
- Herbig G. H., 1975, *ApJ*, 196, 129
- Hobbs G., Lorimer D. R., Lyne A. G., Kramer M., 2005, *MNRAS*, 360, 974
- Hohle M. M., Neuhäuser R., Schutz B. F., 2010, *Astronomische Nachrichten*, 331, 349
- Hoogerwerf R., de Bruijne J. H. J., de Zeeuw P. T., 2001, *A&A*, 365, 49
- Hunter D. A., Massey P., 1990, *AJ*, 99, 846
- Kaper L., van Loon J. T., Augusteijn T., Goudfrooij P., Patat F., Waters L. B. F. M., Zijlstra A. A., 1997, *ApJ*, 475, L37
- Katsuta J. et al., 2012, *ApJ*, 752, 135
- Kenyon S. J., Hartmann L., 1995, *ApJS*, 101, 117
- Kharchenko N. V., 2001, *Kinematika i Fizika Nebesnykh Tel*, 17, 409
- Kirshner R. P., Arnold C. N., 1979, *ApJ*, 229, 147
- Kramer M., Lyne A. G., Hobbs G., Löhmer O., Carr P., Jordan C., Wolszczan A., 2003, *ApJ*, 593, L31
- Kundu M. R., Angerhofer P. E., Fuerst E., Hirth W., 1980, *A&A*, 92, 225
- Lozinskaya T. A., 1976, *SvA*, 20, 19
- Lyne A. G., Lorimer D. R., 1994, *Nat*, 369, 127
- McGowan K. E., Kennea J. A., Zane S., Córdoba F. A., Cropper M., Ho C., Sasseen T., Vestrand W. T., 2003, *ApJ*, 591, 380
- Megier A., Strobel A., Galazutdinov G. A., Krelowski J., 2009, *A&A*, 507, 833
- Milne D. K., 1979, *Australian Journal of Physics*, 32, 83
- Minkowski R., 1958, *Reviews of Modern Physics*, 30, 1048
- Morgan W. W., Code A. D., Whitford A. E., 1955, *ApJS*, 2, 41
- Mugrauer M., Avila G., Guirao C., 2014, *Astronomische Nachrichten*, 335, 417
- Mugrauer M., Berthold T., 2010, *Astronomische Nachrichten*, 331, 449
- Neckel T., Klare G., Sarcander M., 1980, *Bulletin d'Information du Centre de Données Stellaires*, 19, 61
- Ng C.-Y., Romani R. W., Briskin W. F., Chatterjee S., Kramer M., 2007, *ApJ*, 654, 487
- Philp C. J., Evans C. R., Leonard P. J. T., Frail D. A., 1996, *AJ*, 111, 1220
- Poveda A., Ruiz J., Allen C., 1967, *Boletín de los Observatorios Tonantzintla y Tacubaya*, 4, 86
- Przybilla N., Nieva M. F., Heber U., Butler K., 2008, *ApJ*, 684, L103
- Raisbeck G. M., Yiou F., Bourles D., Lorius C., Jouzel J., 1987, *Nat*, 326, 273
- Rieke G. H., Lebofsky M. J., 1985, *ApJ*, 288, 618
- Sallmen S., Welsh B. Y., 2004, *A&A*, 426, 555
- Sauvageot J. L., Ballet J., Rothenflug R., 1990, *A&A*, 227, 183
- Sayer R. W., Nice D. J., Kaspi V. M., 1996, *ApJ*, 461, 357
- Silk J., Wallerstein G., 1973, *ApJ*, 181, 799
- Skiff B. A., 2013, *VizieR Online Data Catalog*, 1, 2023
- Sofue Y., Furst E., Hirth W., 1980, *PASJ*, 32, 1
- Steele I. A., Negueruela I., Clark J. S., 1999, *A&AS*, 137, 147
- Tauris T. M., Takens R. J., 1998, *A&A*, 330, 1047
- Tetzlaff N., Dinçel B., Neuhäuser R., Kovtyukh V. V., 2014, *MNRAS*, 438, 3587
- Tetzlaff N., Eisenbeiss T., Neuhäuser R., Hohle M. M., 2011, *MNRAS*, 417, 617
- Tetzlaff N., Neuhäuser R., Hohle M. M., 2011, *MNRAS*, 410, 190
- Tetzlaff N., Neuhäuser R., Hohle M. M., Maciejewski G., 2010, *MNRAS*, 402, 2369
- Tetzlaff N., Schmidt J. G., Hohle M. M., Neuhäuser R., 2012, 29, 98
- Tetzlaff N., Torres G., Neuhäuser R., Hohle M. M., 2013, *MNRAS*, 435, 879
- van den Bergh S., 1980, *Journal of Astrophysics and Astronomy*, 1, 67
- van den Heuvel E. P. J., 1993, 66, 309
- Walborn N. R., 1971, *ApJS*, 23, 257
- Walborn N. R., Fitzpatrick E. L., 1990, *PASP*, 102, 379
- Wang Z. X., Gies D. R., 1998, *PASP*, 110, 1310
- Wegner W., 1994, *MNRAS*, 270, 229
- Wegner W., 2006, *MNRAS*, 371, 185
- Wongwathanarat A., Janka H.-T., Müller E., 2013, *A&A*, 552, A126
- Woosley S. E., Langer N., Weaver T. A., 1995, *ApJ*, 448, 315
- Zacharias N., Finch C. T., Girard T. M., Henden A., Bartlett J. L., Monet D. G., Zacharias M. I., 2012, *VizieR Online Data Catalog*, 1322, 0
- Zavlin V. E., Pavlov G. G., 2004, 75, 458

This paper has been typeset from a  $\text{\TeX}/\text{\LaTeX}$  file prepared by the author.